LAWRENCE
LIVERMORE
NATIONAL
LABORATORY

LLNL-JRNL-533112

Components of the dilepton continuum in Pb+Pb collisions at sqrt s = 2.76 TeV

R. Vogt, P. Shukla, V. Kumar

February 27, 2012

Physical Review C

Disclaimer

Components of the dilepton continuum in Pb+Pb collisions at $\sqrt{s_{NN}} = 2.76$ TeV

V. Kumar and P. Shukla*
Nuclear Physics Division, Bhabha Atomic Research Center, Mumbai, India and
Homi Bhabha National Institute, Anushakti Nagar, Mumbai, India

R. Vogt
Physics Division, Lawrence Livermore National Laboratory, Livermore, CA 94551, USA and
Physics Department, University of California, Davis, CA 95616, USA

(Dated: February 22, 2012)

The dilepton invariant mass spectrum measured in heavy-ion collisions includes contributions from important QGP probes such as thermal radiation and the quarkonium (J/ψ, ψ' and Υ) states. Dileptons coming from hard $q\overline{q}$ scattering, the Drell-Yan process, contribute in all mass regions. In heavy-ion colliders, such as the LHC, semileptonic decays of heavy flavor hadrons provide a substantial contribution to the dilepton continuum. In the present study, we calculate $c\overline{c}$ and $b\overline{b}$ production and determine their contributions to the dilepton continuum in Pb+Pb collisions at $\sqrt{s_{NN}} = 2.76$ TeV. We also calculate the rates for Drell-Yan and thermal dilepton production. The contributions to the continuum from these dilepton sources are studied in the kinematic ranges relevant for the LHC detectors. The relatively high p_T cutoff for single leptons excludes most dileptons produced by the thermal medium. Heavy flavors are the dominant source of dilepton production in all the kinematic regimes, particularly at forward rapidities, due to the broad rapidity distribution of these decay dileptons.

I. INTRODUCTION

Heavy-ion collisions study the interaction of matter at the extreme temperatures and densities where a Quark-Gluon Plasma (QGP), a phase of nuclear matter dominated by color degrees of freedom, is expected to form. Experimental efforts in this field began with the CERN SPS ($\sqrt{s_{NN}} \sim 16 - 19$ GeV) and evolved with data [1] from the first heavy-ion collider, the Relativistic Heavy-Ion Collider (RHIC) at Brookhaven National Laboratory ($\sqrt{s_{NN}} = 200$ GeV) in the last decade. The advent of Pb+Pb collisions at $\sqrt{s_{NN}} = 2.76$ TeV at the LHC has increased excitement in this field. One of the most striking QGP signals is quarkonium suppression [2]. Quarkonia are identified by their reconstructed mass peaks in the dilepton invariant mass distribution. Below ~ 12 GeV/c^2, the dilepton distribution includes a number of resonance peaks: ρ, ω and ϕ at low masses and the ψ and Υ states at higher masses. At 91 GeV/c^2, the $Z^0 \to l^+l^-$ peak appears. The continuum beneath these resonances is primarily composed of leptons from semileptonic decays of heavy flavor hadrons. These heavy flavor decays not only contribute to the resonance background but are important physics signals in their own right [3–8].

The first measurements of the dilepton spectra at the LHC have recently been reported [9–11]. The CMS experiment reported the first measurements of the Z^0 mass region in Pb+Pb collisions [9] as well as measurements of the full dimuon distribution, including quarkonia [10]. ATLAS has also reported J/ψ and Z^0 measurements in the dimuon channel [11]. The second LHC Pb+Pb run, at much higher luminosity, will provide higher statistics measurements of the dilepton spectra over the full available phase space. With the measurement of dilepton spectrum in Pb+Pb collisions at the LHC, it is time to re-examine the continuum contributions to the dilepton mass spectrum. The production cross sections of $c\overline{c}$ and $b\overline{b}$ pairs at $\sqrt{s_{NN}} = 2.76$ TeV are calculated to next-to-leading order (NLO) and their correlated contributions to the dilepton continuum are subsequently obtained. These contributions are compared to direct dilepton production from the Drell-Yan process and from thermal production in the medium. We then evaluate the relative importance of these contributions in the LHC detector acceptances.

II. DILEPTON PRODUCTION BY HARD PROCESSES

Dilepton production from semileptonic decays of $D\overline{D}$ (charm) and $B\overline{B}$ (bottom) mesons has been an area of active theoretical [4, 5, 7, 12, 13] and experimental [14] research. The large heavy quark mass allows their production to be

*Electronic address: pshukla@barc.gov.in

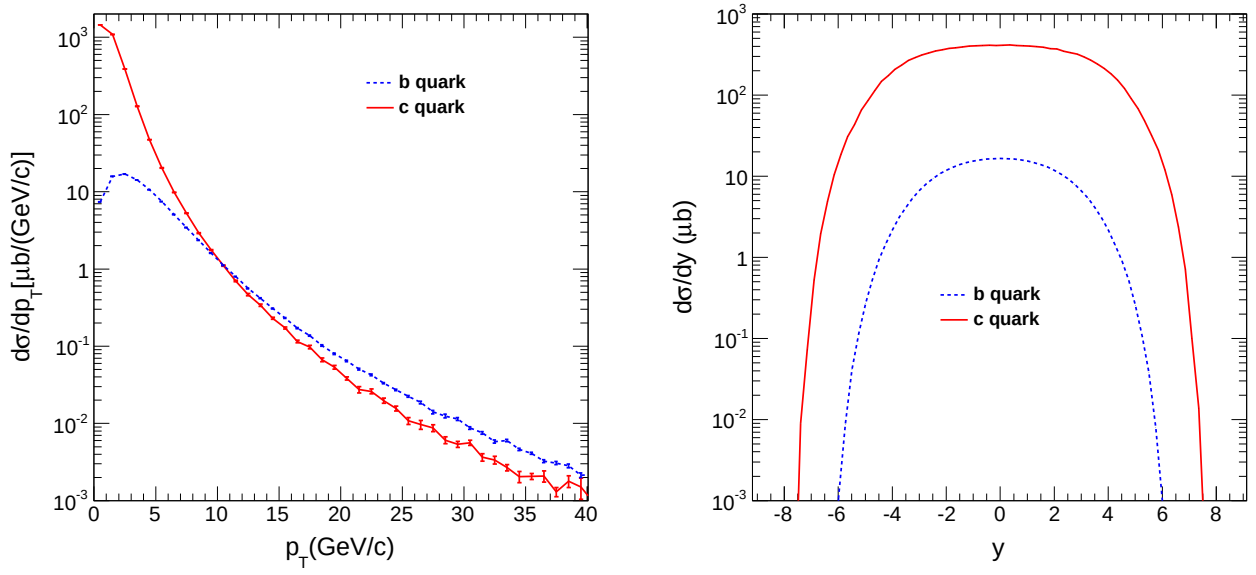

FIG. 1: (Color online) The inclusive single charm and bottom quark per nucleon cross sections as a function of p_T (left) and rapidity (right) in Pb+Pb collisions at $\sqrt{s_{NN}} = 2.76$ TeV. The cross sections, given per nucleon, include modification of the initial parton distributions via the central EPS09 shadowing parameterization.

calculated in perturbative QCD. We calculate the production cross sections for $c\overline{c}$ and $b\overline{b}$ pairs to NLO in pQCD [4, 5] using the CTEQ6M parton densities [15]. The EPS09 parameterization [16] is used to calculate the modifications of the parton densities in Pb+Pb collisions. We use $m_c = 1.2$ GeV/c^2, $\mu_F/m_T = \mu_R/m_T = 2$ for charm production and $m_b = 4.75$ GeV/c^2, $\mu_F/m_T = \mu_R/m_T = 1$ for bottom production where μ_F is the factorization scale, μ_R is the renormalization scale and $m_T = \sqrt{m^2 + p_T^2}$. We note that the uncertainties on the heavy flavor production cross sections can be rather large, see Refs. [17, 18]. Thus the relative charm and bottom rates at 2.76 TeV may vary by a factor of two or more.

The production cross sections for heavy flavour and Drell-Yan dileptons at $\sqrt{s_{NN}} = 2.76$ TeV are shown in Table I. The number of $Q\overline{Q}$ pairs in a minimum bias Pb+Pb event is obtained by multiplying the per nucleon cross section, $\sigma_{\rm PbPb}$, by the nuclear overlap function [19] for minimum bias Pb+Pb collisions,

$$N_{Q\overline{Q}} = \sigma_{\rm PbPb} T_{\rm PbPb} \ . \tag{1}$$

At 2.76 TeV the total Pb+Pb cross section is 7.65 b [20] so that $T_{\rm PbPb} = 5.65$ mb^{-1}.

Figure 1 gives the p_T (left) and rapidity (right) spectra of single inclusive charm and bottom quark production cross section per nucleon in Pb+Pb collisions at $\sqrt{s_{NN}} = 2.76$ TeV. The differences in the p_T distributions are primarily at low p_T, $p_T \leq m_b$. At $p_T \gg m_b$, the p_T distributions are very close to each other. The widths of the rapidity distributions are limited by the heavy quark mass. Thus the charm rapidity distribution is broader than that for bottom.

We assume that all the observed heavy flavor production in Pb+Pb collisions occurs during the initial nucleon-nucleon collisions. Thermal production of $Q\overline{Q}$ pairs is expected to be only a fraction of this initial production [4] unless the plasma is composed of massive quasi-particles which would lower the effective threshold for heavy flavor production in the medium [21], enhancing production in this channel. However, such production would be at lower transverse momentum and with a narrower rapidity distribution than shown in Fig. 1.

The heavy quarks are decayed semileptonically and lepton pairs are formed from correlated $Q\overline{Q}$ pair decays. We do not consider uncorrelated $Q\overline{Q}$ contributions to the continuum since these should be eliminated by a like-sign subtraction. We assume that any uncorrelated dileptons from $c\overline{b}$ and $\overline{c}b$ decays are also removed by like-sign subtraction and that lepton pairs from a single chain decay, $B \to Dl_1X \to l_1l_2X'$, only contribute to the low mass continuum, see Ref. [6]. The number of lepton pairs is obtained from the number of $Q\overline{Q}$ pairs,

$$N_{\mu^+\mu^-} = N_{Q\overline{Q}}[B(Q \to lX)]^2 \ . \tag{2}$$

The values of $N_{Q\overline{Q}}$ and $N_{\mu^+\mu^-}$ can also be found in Table I.

TABLE I: Heavy flavor and Drell-Yan cross sections at $\sqrt{s_{NN}} = 2.76$ TeV. The cross sections are given per nucleon while $N_{Q\overline{Q}}$ and $N_{l^+l^-}$ are the number of $Q\overline{Q}$ and lepton pairs per Pb+Pb event.

	$c\overline{c}$	$b\overline{b}$	DY
			$1 \leq M \leq 100$ GeV
$\sigma_{\rm PbPb}$	3.15 mb	89.25 μb	70.97 nb
$N_{Q\overline{Q}}$	17.55	0.50	-
$N_{\mu^+\mu^-}$	0.19	0.0059	0.0004

Dilepton production in the Drell-Yan process has also been calculated to NLO in pQCD [22]. The cross section in the mass interval $1 < M < 100$ GeV, including EPS09 shadowing in Pb+Pb collisions, is given in Table I. The integrated cross section is dominated by the lowest masses. The largest potential modification due to the presence of the nucleus is on the low mass rate, in the resonance region. At larger masses, this effect becomes competitive with the effects of the relative number of protons and neutrons in the nucleus compared to a pp collision (isospin effects) [23]. We have used PYTHIA [24] to generate the Drell-Yan p_T distribution and to place kinematic cuts on the individual leptons of the pair. The total rate has been normalized to the NLO cross section. The pQCD uncertainties on the Drell-Yan rate, particularly above the resonance region, are not large. In general, they are smaller than the uncertainties due to the shadowing parameterization [23].

Finally, we remark that we have not considered energy loss effects on the heavy quarks. Since they do not decay until after they have traversed the plasma, their contribution to the final dilepton spectra will reflect the influence of the media. Indications from non-photonic single leptons at RHIC, attributed to heavy flavor decays, suggest that the effects of energy loss are strong and persist up to high p_T. They also suggest that the magnitude of the loss is similar for that of light flavors, *i.e.* independent of the quark mass. These effects are still under investigation, see Ref. [25] and references therein.

III. THERMAL DILEPTON PRODUCTION

The contribution of thermal dileptons is calculated assuming that a QGP is formed in local thermal equilibrium at some initial temperature T_i and initial time τ_i which cools hydrodynamically through a 1D Bjorken expansion [26]. Assuming a first-order phase transition, when the QGP cools to the critical temperature T_c at time τ_c, the temperature of the system is held fixed until hadronization is completed at time τ_h. Afterwards, the hadron gas cools to the freeze-out temperature T_f at time τ_f [27].

The thermal dilepton emission rate due to $q\overline{q} \to l^- l^+$ is [27, 28]

$$\begin{aligned} \frac{dN}{d^4x d^2p_T dy dM^2} &= \frac{3}{(2\pi)^5} M^2 \sigma(M^2) F \exp(-E/T) \\ &= \frac{\alpha^2}{8\pi^4} F \exp(-E/T) \ . \end{aligned} \tag{3}$$

Here M, p_T and y are the mass, transverse momentum, and rapidity of the lepton pair while $d^4x = \tau d\tau \eta \pi R_A^2$ where η is the rapidity of the fluid with temperature T and $R_A = r_0 A^{1/3}$. The mass-dependent cross section, $\sigma(M^2) = F\ 4\pi\alpha^2/3M^2$ includes a factor F that depends on the phase of the matter. In a two-flavor QGP, $F_{\rm QGP} = \sum e_q^2 = 5/9$, while, in the hadronic phase, form factors representing the resonance region [29], are used. We concentrate on masses above the resonance region. In the mixed phase,

$$F = (1 - h(\tau))\, F_{\rm QGP} + h(\tau)\, F_{\rm had} \ , \tag{4}$$

where $h(\tau)$ is the hadron fraction of the mixed phase.

The dilepton p_T distribution is

$$\frac{dN}{d^4x dy dM dp_T} = \frac{\alpha^2}{4\pi^4} F\, M\, p_T\, \exp\left(-\frac{\sqrt{M^2 + p_T^2}\cosh(y-\eta)}{T} \right) \tag{5}$$

and the dilepton invariant mass distribution, integrated over p_T, is

$$\frac{dN}{d^4x dy dM} = \frac{\alpha^2}{2\pi^3} F\, M^3 \left(\frac{1}{x^2} + \frac{1}{x} \right) \exp(-x), \tag{6}$$

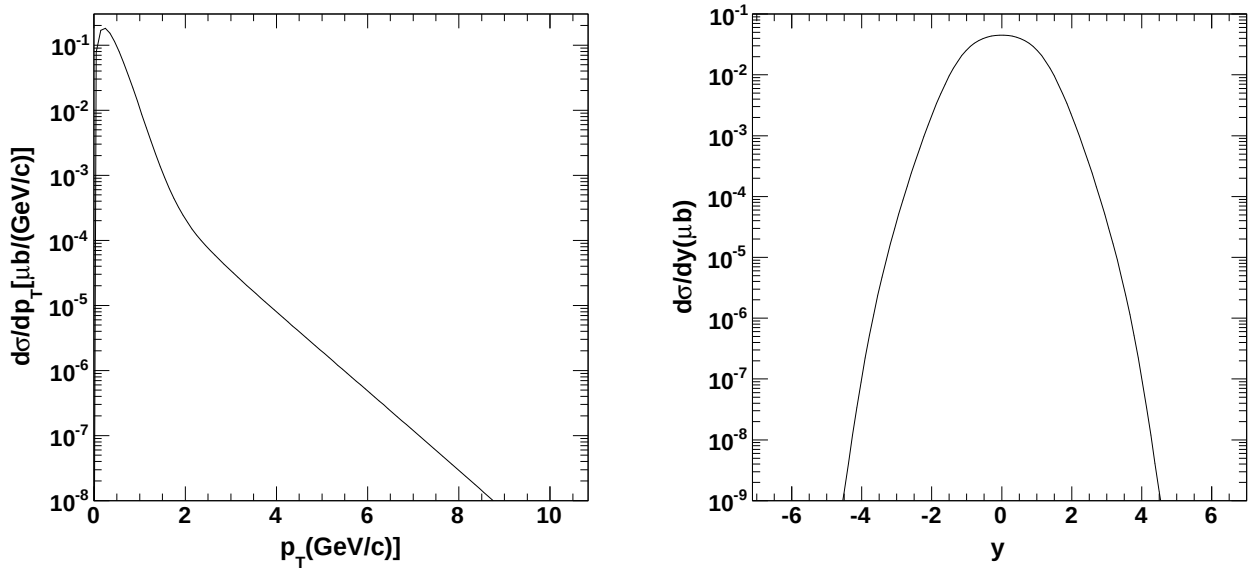

FIG. 2: The thermal dilepton cross section as a function of p_T (left) and rapidity (right) in Pb+Pb collisions at $\sqrt{s_{NN}} = 2.76$ TeV.

where

$$x = \frac{M \cosh(y - \eta)}{T}. \tag{7}$$

The initial time is assumed to be $\tau_i = 0.1$ fm/c. The initial temperature T_i is obtained from the total multiplicity distribution,

$$\frac{dN}{dy} = \tau_i T_i^3 4 a_q \pi R_A^2 / 3.6 \ , \tag{8}$$

where $dN/dy = 1.5\ dN_{\rm ch}/dy$. The charged particle multiplicity, $dN_{\rm ch}/dy = 1600$, was measured in Pb+Pb collisions at 2.76 TeV [30]. Using this value with $a_q = 37\pi^2/90$ gives $T_i = 636$ MeV. The temperature decreases in the QGP as

$$T(\tau) = T_i \left(\frac{\tau_i}{\tau}\right)^{1/3} \tag{9}$$

for $\tau_i < \tau < \tau_c$. The temperature in mixed phase is $T = T_c = 160$ MeV. The mixed phase ends at $\tau_h = (a_q/a_h)\tau_c$ where $a_h = 3\pi^2/90$ for a pion gas. The hadronic fraction of the mixed phase, $h(\tau)$, is

$$h(\tau) = \frac{a_q}{a_q - a_h} \left(\frac{\tau - \tau_c}{\tau}\right) \ . \tag{10}$$

The temperature in hadron phase between $\tau_h < \tau < \tau_f$, is

$$T(\tau) = T_c \left(\frac{\tau_h}{\tau}\right)^{1/3} \ . \tag{11}$$

The thermal dilepton rate given in Eqs.(5) and (6) is converted to a cross section by dividing the rate by the minimum bias nuclear overlap, $T_{\rm PbPb}$. Figure 2 shows the differential cross sections for thermal dilepton production as a function of p_T and rapidity. The p_T distribution, integrated over pair mass, shows two slopes, a steep decrease when the minimum pair transverse mass, M_T, is on the order of the temperature and a long tail when $M_T \gg T$. The rapidity distribution is significantly narrower than those resulting from the initial hard scatterings shown in Fig. 1.

This simple application of a one-dimensional Bjorken expansion through a first-order phase transition significantly overestimates the lifetime of the hot system. Thus, the results shown in Fig. 2 should be regarded as an upper limit on the thermal contribution.

To obtain the pair mass distributions including single lepton cuts, single leptons are generated by a Monte Carlo based on the pair M, p_T and y distributions using energy-momentum conservation.

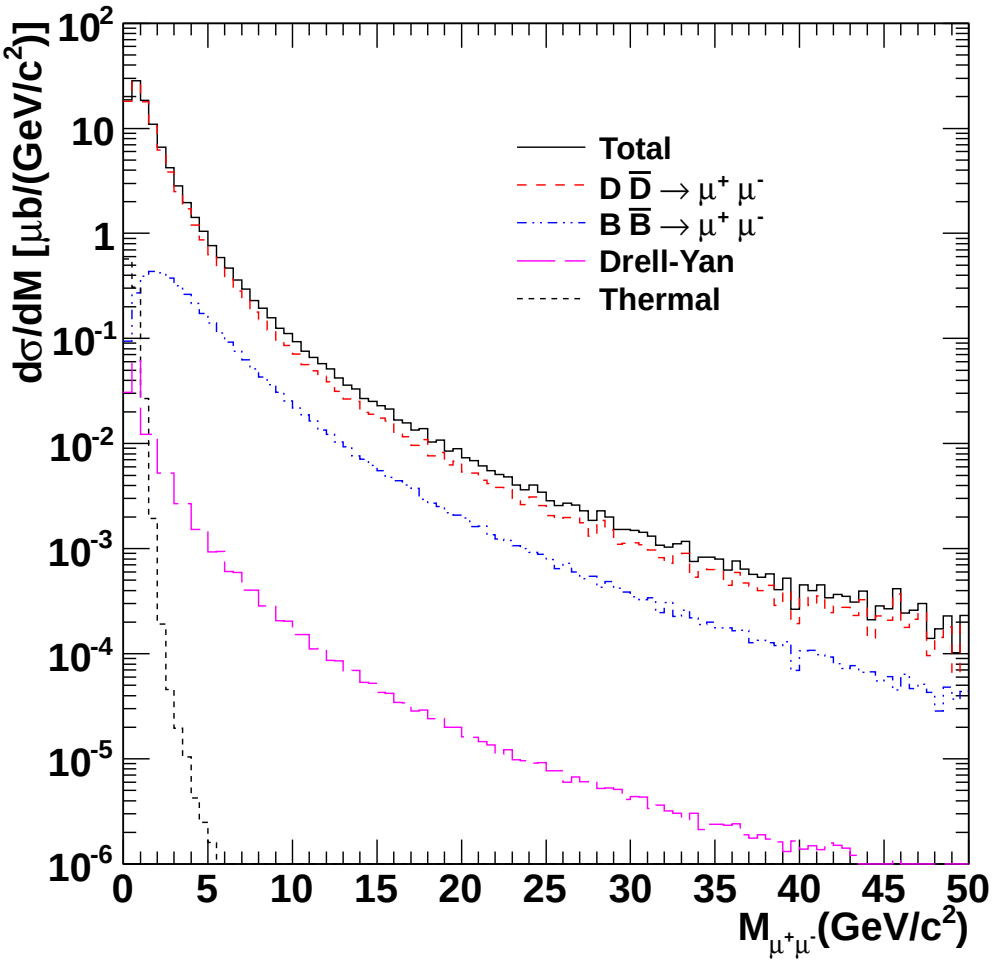

FIG. 3: (Color online) The invariant mass distributions for the four contributions to the dilepton spectra discussed here: semileptonic charm (red, short-dashed) and bottom (blue, dot-dot-dashed) decays, Drell-Yan (magenta, long-dashed) and thermal (black, dotted) dileptons along with the sum (black, solid) in Pb+Pb collisions per nucleon pair at $\sqrt{s_{NN}} = 2.76$ TeV. The per nucleon cross sections are given. No phase space or kinematic cuts are introduced.

IV. RESULTS AND DISCUSSION

Figure 3 shows the dimuon invariant mass distributions from each of the four sources considered: semileptonic decays of correlated $Q\overline{Q}$ pairs and direct production of Drell-Yan and thermal dileptons in Pb+Pb collisions at $\sqrt{s_{NN}} = 2.76$ TeV. No kinematic cuts are included. Without any cuts, dileptons from $D\overline{D}$ decays dominate over the entire mass range due to the large $c\overline{c}$ production cross section. Bottom pair decays are the next largest contribution followed by Drell-Yan production. At masses below 3 GeV/c^2, the Drell-Yan and thermal dilepton contributions are competitive. Otherwise, the thermal contribution is negligible.

We now examine these distributions in the kinematic regimes appropriate for the LHC detectors. CMS [31] and ATLAS [32] have excellent muon detectors with similar coverage in the central rapidity region, $|\eta^\mu| \leq 2.4$. However, due to the large magnetic fields, only muons above a rather high minimum p_T, $p_T > 3.0$ GeV/c, make it into the muon detectors. ALICE [33] has muon acceptance on one side of the forward rapidity region, $2.5 \leq \eta^\mu \leq 4.0$. At central rapidities, $|\eta^\mu| \leq 1.0$, ALICE has an electron detector. While there have been previous studies of Pb+Pb collisions at 5.5 TeV [4, 6, 34], a re-examination is appropriate at the current, lower, center of mass energy and with the final detector acceptances.

Figure 4 shows the dimuon invariant mass distribution for single muons in the range $|\eta^\mu| \leq 2.4$, together with several muon p_T cuts. Figure 4(a) has no muon p_T cut, only the η cut. Comparison with Fig. 3 shows that the

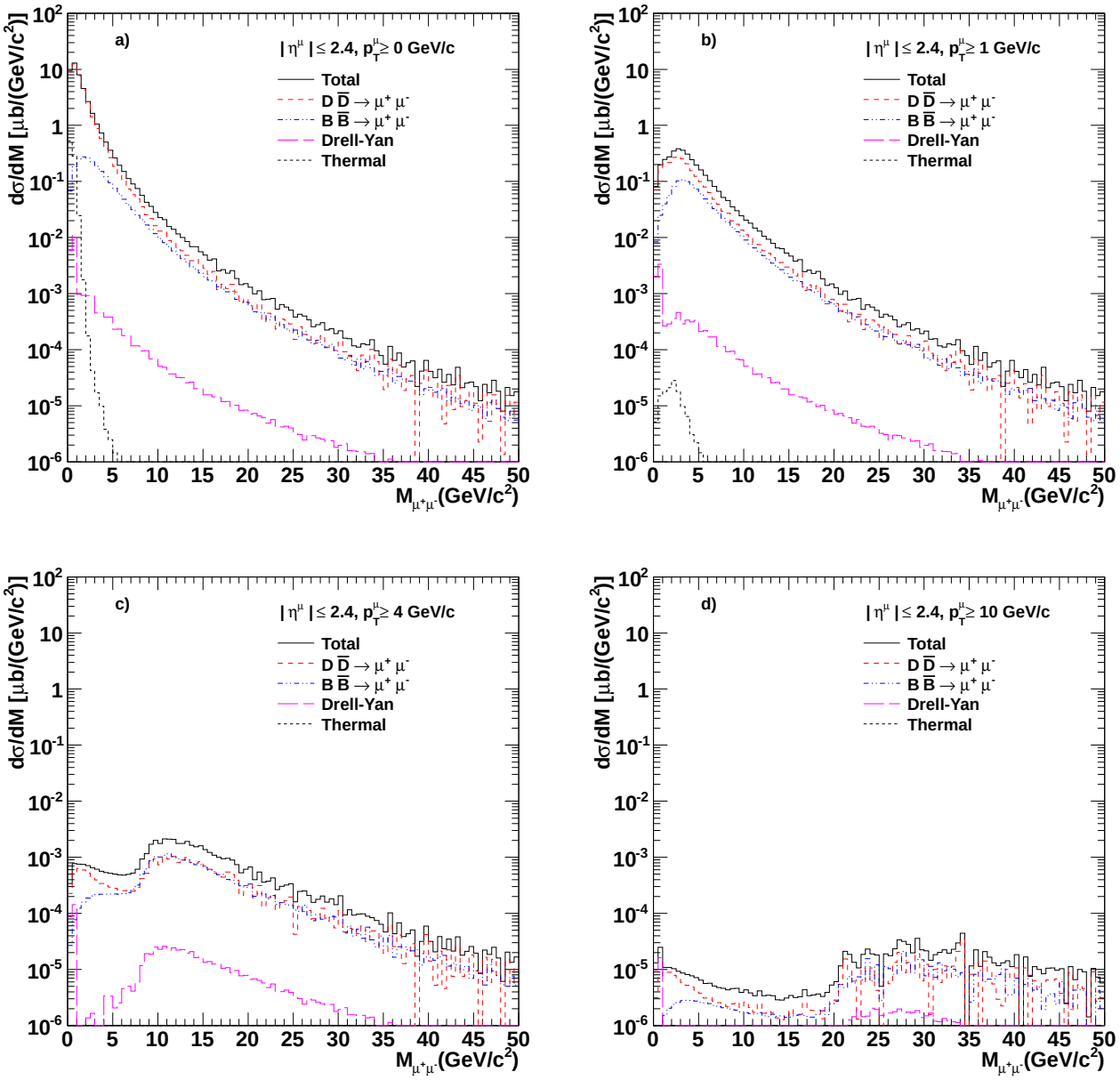

FIG. 4: (Color online) The same as Fig. 3 but now with single muon rapidity cuts of $|\eta^{\mu}| \leq 2.4$. A minimum single lepton transverse momentum cut of $p_T^{\mu} \geq 0$ (a), 1 (b), 4 (c) and 10 (d) GeV/c is also shown.

thermal dilepton contribution is almost unaffected since the width of its rapidity distribution is small enough to fit within the CMS rapidity acceptance. Since the Drell-Yan rapidity distribution narrows with increasing mass, only the low mass region is affected by the rather broad rapidity cut of $|\eta^{\mu}| \leq 2.4$. Because the charm rapidity range is broader than that of bottom production, the dileptons from charm decays are most affected by the rapidity cut. For $M_{\mu^+\mu^-} > 10$ GeV/c^2, the two contributions are essentially on top of each other and the high mass continuum is composed of almost equal parts charm and bottom production.

Adding a cut on single lepton p_T disproportionally affects the low mass part of the continuum. As the minimum lepton p_T is increased from 1 GeV/c to 10 GeV/c in Figs. 4(b)-4(d), an ever-deepening dip appears in the dilepton mass distribution for $M_{\mu^+\mu^-} < 2p_T^{\mu}$. Even a relatively low p_T cut essentially eliminates the thermal dilepton contribution since these leptons have a rather soft p_T distribution. Since the charm and bottom quark p_T distributions have the same slope for $p_T > 10$ GeV/c, their decays are affected the same way by the lepton p_T cut. Thus, above masses of ~ 10 GeV/c^2 the two contributions are effectively equivalent. We note that the statistical significance of the charm

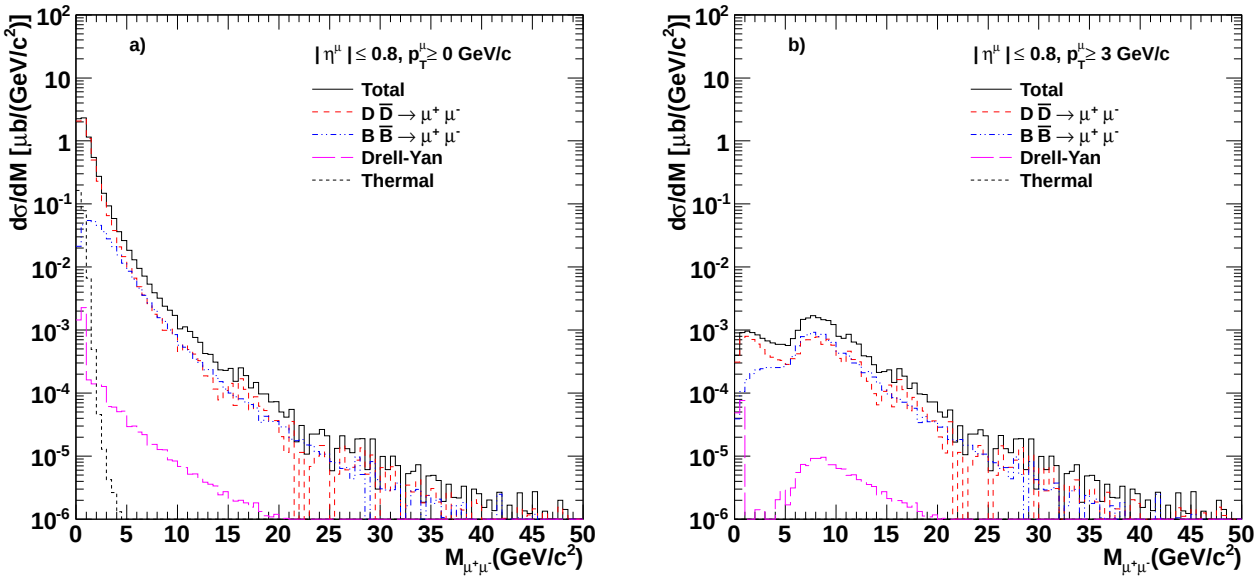

FIG. 5: (Color online) The same as Fig. 3 but now with single muon rapidity cuts of $|\eta^{\mu}| \leq 0.8$. A minimum single lepton transverse momentum cut of $p_T^{\mu} \geq 0$ (a) and 3 (b) GeV/c is also shown.

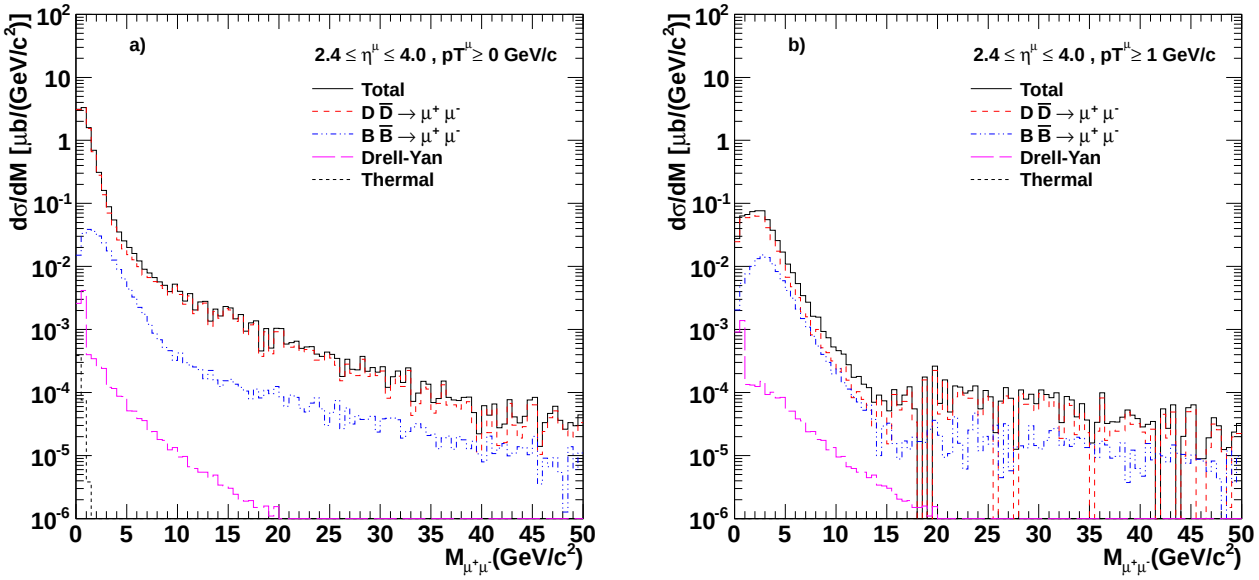

FIG. 6: (Color online) The same as Fig. 3 but now with single muon rapidity cuts of $2.4 \leq |\eta^{\mu}| \leq 4$. A minimum single lepton transverse momentum cut of $p_T^{\mu} \geq 0$ (a) and 1 (b) GeV/c is also shown.

decay contribution is reduced relative to bottom decays, causing greater fluctuations at higher dilepton masses. We note that the single lepton cut of $p_T^{\mu} > 10$ GeV/c, published with the CMS Z^0 measurement [9] and corresponding to approximately 50 million events, had a very small continuum background.

Figure 5 shows the dimuon mass distribution in the narrower rapidity interval $|\eta^{\mu}| \leq 0.8$, equivalent to the muon acceptance of the CMS barrel region and similar to the ALICE electron acceptance $|\eta^{e}| \leq 1.0$. Figure 5(a) shows the dimuon distribution without any p_T cut. In this case, the mass distribution is more steeply falling in all cases except for thermal dilepton production due to its narrow rapidity distribution. Since the heavy flavor hadrons decay isotropically to leptons, the rapidity distribution for lepton pairs is rather broad with a width that is not strongly

dependent on the pair mass. Thus the narrower rapidity acceptance reduces the high mass yields substantially relative to Fig. 4, even before any single lepton p_T cuts. Adding a single lepton transverse momentum cut of $p_T^\mu > 3$ GeV/c, Fig. 5(b), suppresses the low mass part of the distribution. However, the mass distribution is essentially unaffected by the p_T^μ cuts for $M_{\mu^+\mu^-} > 8$ GeV/c^2.

Figure 6 shows the dimuon mass distributions in the forward region, $2.5 \leq \eta^\mu \leq 4.0$, relevant for the ALICE muon arm without any p_T cut. In this case, there is a clear separation between the charm and bottom decay contributions over the entire mass range. This is due to the nature of the lepton decay kinematics. While the heavy flavor production kinematics favors central production, with a rather steep decrease in the rapidity distribution as the kinematic limit is approached, there is no such constraint on the resulting lepton pairs. Because the decay of the individual heavy quark is isotropic in its rest frame, the lepton rapidity distribution has a larger plateau region, extending to more forward rapidity, than the parent quark. The final lepton pair rapidity distribution is a weaker function of rapidity than the initial heavy quark pair. This holds for high mass lepton pairs as well, particularly when there is no lepton p_T cut. However, because the rapidity distribution of lepton pairs from bottom decays is somewhat narrower than those from charm decays, there is a visible distinction between the two in the forward region, sufficient to result in clear separation between the charm and bottom contributions here. The high mass contribution is much larger than in the narrower central region shown in Fig. 5 due to the larger rapidity gaps between the decay leptons. A narrow central rapidity coverage will not accept either one or both of such large rapidity gap dileptons. As a minimum lepton p_T is introduced, this separation is washed out, as is the flatter shape of the dilepton mass distribution, dropping more steeply for minimum p_T values greater than the 1 GeV/c shown in Fig. 6(b). Very little remains of the thermal dilepton contribution in the forward region due to its narrow rapidity distribution. The high mass Drell-Yan contribution is similarly affected. We note, however, that more of the low mass contribution is retained at forward rapidity than in the narrower central region shown in Fig. 5(a).

The present study gives insight into importance of the contributions to the dilepton continuum in the kinematic regions relevant for the LHC detectors. Since most detectors accept only high p_T single leptons, thermal dileptons would be difficult to measure. In most of the kinematic regions considered, the charm and bottom decay contributions are equivalent for lepton pair masses greater than 10 GeV/c^2. At forward rapidity, as in Fig. 6, the charm and bottom contributions are much larger at high masses due to the greater rapidity gaps between the decay leptons. Thus, the ALICE muon arm can measure the heavy flavor continuum quite well. This contribution also provides a larger background for Υ measurements. From the approximately 50 M events collected by CMS in the first year of Pb+Pb collisions, we conclude that there will be few continuum contributions above 40 GeV/c^2, evident from the high mass dimuon distribution published by the CMS [9], in agreement with the result shown in Fig. 4(d). The second Pb+Pb run in 2011 has 20 times more events which will help in quantifying the heavy flavour contribution. When comparing calculations such as these with the data, a scheme to eliminate uncorrelated pairs such as like-sign subtraction should be employed. The effects of energy loss on the decay dileptons will alter their acceptance, particularly for high lepton p_T cuts. However, their relative contributions should remain similar, especially at high pair masses [6].

V. ACKNOWLEDGMENTS

The authors are grateful to Dr. D. K. Srivastava for many fruitful discussions. The work of R.V. was performed under the auspices of the U.S. Department of Energy by Lawrence Livermore National Laboratory under Contract DE-AC52-07NA27344 and supported within the framework of the JET Collaboration.

[1] I. Arsene *et al.* (BRAHMS Collaboration), Nucl. Phys. A **757**, 1 (2005); B. B. Back *et al.* (PHOBOS Collaboration), Nucl. Phys. A **757**, 28 (2005); J. Adams *et al.* (STAR Collaboration), Nucl. Phys. A **757**, 10 (2005); K. Adcox *et al.* (PHENIX Collaboration), Nucl. Phys. A **757**, 184 (2005).
[2] T. Matsui and H. Satz, Phys. Lett. B 178, **416** (1986).
[3] N. Armesto *et al.*, J. Phys. G **35**, 054001 (2008).
[4] S. Gavin, P. L. McGaughey, P. V. Ruuskanen, and R. Vogt, Phys. Rev. C **54**, 2606 (1996).
[5] Z. Lin, R. Vogt and X. N. Wang, Phys. Rev. C **57**, 899 (1998).
[6] Z. Lin and R. Vogt, Nucl. Phys. B **544**, 339 (1999).
[7] E. Shuryak, Phys. Rev. C **55**, 961 (1997).
[8] U. Jamil and D. K. Srivastava, J. Phys. G **37**, 085106 (2010).
[9] S. Chatrchyan *et al.* (CMS Collaboration), Phys. Rev. Lett. **106**, 212301 (2011)
[10] CMS collaboration, arXiv:1201.5069v1 [nucl-ex]; CMS-HIN-10-006.
[11] G. Aad *et al.* (ATLAS Collaboration), arXiv:1012.5419 [hep-ex] (2010).

[12] D. Fein, Z. Huang, P. Valerio and I. Sarcevic, Phys. Rev. C **56**, 1637 (1997).
[13] M. G. Mustafa, D. Pal and D. K. Srivastava, Phys. Rev. C **57**, 889 (1998).
[14] H. Agakishiev *et al.* (STAR Collaboration), Phys. Rev. D **83**, 052006 (2011) [arXiv:1102.2611 [nucl-ex]]; A. Adare *et al.* (PHENIX Collaboration), Phys. Rev. Lett. **97**, 252002 (2006) [hep-ex/0609010].
[15] J. Pumplin, D. R. Stump, J. Huston, H. L. Lai, P. M. Nadolsky and W. K. Tung, JHEP **0207**, 012 (2002) [arXiv:hep-ph/0201195]; D. Stump, J. Huston, J. Pumplin, W. K. Tung, H. L. Lai, S. Kuhlmann and J. F. Owens, JHEP **0310**, 046 (2003) [arXiv:hep-ph/0303013].
[16] K. J. Eskola, H. Paukkunen and C. A. Salgado, JHEP **0904**, 065 (2009) [arXiv:0902.4154 [hep-ph]].
[17] R. Vogt, Eur. Phys. J. Special Topics **155**, 213 (2008).
[18] R. Vogt, Eur. Phys. J. C **61**, 793 (2009).
[19] D. d'Enterria, arXiv:nucl-ex/0302016v3 (2004).
[20] S. Chatrchyan *et. al.* (CMS Collaboration), Phys. Rev. C **84**, 024906 (2011).
[21] P. Lévai and R. Vogt, Phys. Rev. C **56**, 2707 (1997).
[22] R. Hamberg, W.L. van Neerven and T. Matsuura, Nucl. Phys. **B359**, 343 (1991).
[23] A. Accardi *et al.*, arXiv:hep-ph/0308248.
[24] T. Sjöstrand, S. Mrenna and P. Skands, JHEP **05**, 026 (2006) [arXiv:hep-ph/0603175].
[25] A. D. Frawley, T. Ullrich and R. Vogt, Phys. Rept. **462**, 125 (2008) [arXiv:0806.1013 [nucl-ex]].
[26] J. D. Bjorken, Phys. Rev. D **27**, 140 (1983).
[27] K. Kajantie, M. Kataja, L. McLerran, and P. V. Ruuskanen, Phys. Rev. D **34**, 811 (1986).
[28] R. Vogt, B. V. Jacak, P. L. McGaughey, P. V. Ruuskanen, Phys. Rev. D **49**, 3345 (1994).
[29] C. Gale and P. Lichard, Phys. Rev. D **49**, 3338 (1994);
C. Song, C.M. Ko, and C. Gale, *ibid* **50** R 1827 (1994).
[30] S. Chatrchyan *et al.* (CMS Collaboration), arXiv:1107.4800 [nucl-ex] (2011).
[31] S. Chatrchyan *et al.* (CMS Collaboration), JINST **3**, S08004 (2008).
[32] ATLAS Collaboration, JINST **3**, S08003 (2008).
[33] ALICE Collaboration, Technical Proposal, CERN/LHCC/95-71; The ALICE Collaboration, JINST **3**, S08002 (2008).
[34] K. Gallmeister, B. Kampfer, and O. P. Pavlenko, Phys. Rev. C **57**, 3276 (1998).